Orientation fluctuation-induced spinodal decomposition in polymer–liquid-crystal mixtures

Akihiko Matsuyama,* R. M. L. Evans, and M. E. Cates
Department of Physics and Astronomy, The University of Edinburgh, JCMB King's Building, Mayfield Road, Edinburgh EH9 3JZ, Scotland, United Kingdom
(Received 4 October 1999)

We study the early stages of spinodal decomposition (SD) in polymer–liquid-crystal mixtures by solving linearized time-dependent Landau-Ginzburg equations for concentration (conserved order parameter) and orientation (nonconserved order parameter). The theory takes into account a cross term between concentration and orientation gradients, which becomes an important factor for phase separation kinetics. We calculate structure factors for concentration and for orientation, depending on a quench temperature and concentration. We find a new SD process driven by instability of the orientational order parameter. In this case, the average domain size initially grows as a nontrivial and evolving power of time, which starts as $t^{1/3}$ in our minimal model. The domain growth is advanced by the coupling between the two order parameters.

PACS number(s): 64.75.+g, 61.30.Gd, 61.25.Hq

I. INTRODUCTION

A homogeneous binary mixture quenched from a stable into a thermodynamically unstable state within a phase diagram develops into an inhomogeneous one. Among the various kinetic mechanisms, spinodal decomposition (SD) is induced by the instability of the order parameter (usually concentration) which describes the system [1]. In the early stages, the SD is interpreted within the framework of the Cahn theory for isotropic systems [2–4]. On the other hand, in the late stages, the SD is limited by diffusionlike processes (or by hydrodynamics, which we do not treat) and exhibits slow coarsening. In this diffusive coarsening regime, the domains of the conserved order parameter grow as $t^{1/3}$ with time t [3,5]. On the other hand, for the case of a nonconserved order parameter such as the polarization of a ferroelectric solid, we may have the $t^{1/2}$ law [3,6]. In polymer–liquid-crystal mixtures, we can expect co-occurrences between phase separation and liquid crystalline ordering such as nematic and smectic phases. Such inhomogeneous materials, described by one conserved order parameter (concentration) and one nonconserved order parameter (orientational order parameter) are important for not only fundamental scientific reasons but also technological applications in high modulus fiber and electro-optical devices [7,8].

In polymer–liquid-crystal mixtures [9–18], biphasic regions between an isotropic and a nematic phase appear below the nematic-isotropic transition (NIT) temperature of the pure liquid-crystal molecule (mesogen). When the system is thermally quenched from a stable isotropic phase into an unstable part of the biphasic region, the fluctuations of concentration and of orientation take place and isotropic or nematic droplets appear with time [19,20]. The instability of these systems is driven by the competition between phase separation and nematic ordering.

To elucidate the time evolution of the concentration and orientation fluctuations during the spinodal decomposition, we calculate the structure factor for concentration and for orientation using time-dependent Landau-Ginzburg (TDLG) equations for concentration and orientational order parameters [4,21–27]. Some years ago, Dorgan expressed the structure factors for concentration and for orientation in mixtures containing nematogens in term of the linearized TDLG [24]. Recently Chiu and Kyu simulated the dynamics of phase separations in polymer–liquid-crystal mixtures [25]. However, these theories eliminate the cross term between the gradients of the two order parameters. Some authors have shown that this cross term plays a significant role on phase separation kinetics of solutions containing liquid crystals or liquid-crystalline polymers [26–28]. In this paper we take into account the cross term and calculate the structure factor for concentration and for orientation using the linearized TDLG. The aim of this paper is to study the early stages of the SD. Depending on the concentration of liquid crystal, we find two types of SD. We discuss the possible mechanisms for formations of nematic droplets under the SD processes. We also show simulations in one dimension (but without linearization) to further understand our analytical results for the structure factors.

II. PHASE DIAGRAMS OF POLYMER–LIQUID-CRYSTAL MIXTURES

In this section we introduce the free energy to describe the static phase diagrams. There are many theories to describe the phase behaviors of polymer–liquid-crystal mixtures [13–18]. We here focus on sufficiently flexible polymer chains and so we neglect the orientational ordering of the polymer chains. In this paper we use for simplicity the Landau expansion form for the nematic free energy [18,29]. The dimensionless equilibrium free energy density $f(\phi,S)$ of polymer–liquid-crystal mixtures is given by combining the Flory-Huggins theory [30] for isotropic mixing of two components with the Maier-Saupe theory for nematic ordering [29,31,32]:

*Permanent address: Department of Chemistry for Materials, Faculty of Engineering, Mie University, Tsu Mie 514, Japan.

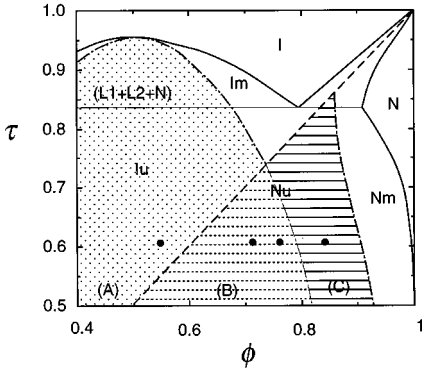

FIG. 1. Phase diagram of a polymer–liquid-crystal mixture with $n_p=n_l=2$ and $\nu/\chi=1.4$. The solid curve refers to the binodal and the dotted line shows the first-order NIT line. The dash-dotted line shows the spinodal. Filled circles indicate temperature quenches from the stable isotropic phase into the isotropic unstable (Iu; A) and nematic unstable (Nu; B, C) regions.

$$f(\phi,S)=\frac{1-\phi}{n_p}\ln(1-\phi)+\frac{\phi}{n_l}\ln\phi+\chi\phi(1-\phi)+\nu\phi^2\left[\frac{1}{2}\left(1-\frac{\eta}{3}\right)S^2-\frac{\eta}{9}S^3+\frac{\eta}{6}S^4\right], \quad (2.1)$$

where ϕ is the volume fraction of the liquid crystals and S is the ''scalar'' orientational order parameter of the liquid crystals discussed further below, n_p is the number of segments on the polymer, n_l is axis ratio of the liquid crystal molecule, and $\eta\equiv n_l\nu\phi$. The value $\chi(\equiv U_0/k_BT)$ is the Flory-Huggins interaction parameter related to isotropic interactions between unlike molecular species and $\nu(\equiv U_a/k_BT)$ parametrizes the orientation-dependent (Maier-Saupe) interactions between the mesogens [32]. The coexistence (binodal) curve of the phase equilibrium is derived by a double tangent method where the equilibrium volume fractions fall on the same tangent line to the free energy curve. The spinodal line, which separates metastable from unstable compositions, is given by the inflection point of the free energy $(\partial^2 f/\partial\phi^2)_T=0$.

A typical phase diagram on the temperature-concentration plane is shown in Fig. 1 which is calculated with $n_p=n_l=2$ and $\nu/\chi=1.4$ [18]. The reduced temperature τ $(\equiv T/T_{NI}^\circ)$ is normalized by the nematic-isotropic transition (NIT) temperature T_{NI}° of the pure liquid crystal (at $\phi=1$). According to Eq. (2.1), this temperature is given by $T_{NI}^\circ=3n_lU_a/8k_B$ where the nematic phase has $S=0.25$ [29]. The critical solution point in the isotropic phase is at $\phi=0.5$ and $\tau=0.95$. The solid curve refers to the binodal and the dotted line shows the first-order NIT of a hypothetical homogeneous phase. The dash-dotted line shows the spinodal. Note that the origin is suppressed on the ϕ axis. When $\tau=0.831$, we have a triple point where two isotropic liquid phases (L_1+L_2) and a nematic phase (N) can simultaneously coexist. Below the triple point, we have the two-phase coexistence between an isotropic and a nematic phase. Such phase diagrams are observed in mixtures of *n*-tetracosane and nematic liquid crystal [11]. In the biphasic region between the nematic and the isotropic phases, we have two different metastable regions: an isotropic metastable (Im) and a nematic metastable (Nm), and two unstable regions: an isotropic unstable (Iu; A) and a nematic unstable (Nu; B, C) [16–18]. On increasing the molecular weight n_p of the polymer, the critical solution point shifts to higher temperatures and higher concentrations of mesogens and the Nu and Iu regions also shift to higher temperatures and higher concentrations with increasing n_p [16–18].

Filled circles indicate temperature quenches from the stable isotropic phase into the isotropic unstable (Iu; A) and nematic unstable (Nu;B, C) regions. The region (A), lying below the isotropic spinodal curve and above the NIT line, corresponds to a system which is initially unstable with respect to concentration fluctuations, but metastable to orientation fluctuations. The region (B), between the isotropic spinodal curve and the NIT line, is initially unstable to both concentration and orientation fluctuations. In the region (C) between the isotropic spinodal curve and the nematic spinodal curve, the system is initially unstable with respect to orientation fluctuations, but metastable to concentration fluctuations. Thus if we thermally quench from an isotropic phase to these different regions, we can expect a variety of SD processes even in the early stages. In the next section we consider the phase separation dynamics for two order parameters appropriate to this problem.

III. KINETIC EQUATIONS

We consider polymer-mesogen mixtures described by one conserved order parameter (volume fraction ϕ of mesogen) and one nonconserved order parameter (orientational order parameter S_{ij}). Since the orientational order parameter is a traceless symmetric tensor, its components can be expressed as [33,34]

$$S_{ij}=\frac{3}{2}S(r)\left(n_i(r)n_j(r)-\frac{1}{3}\delta_{ij}\right), \quad (3.1)$$

where $i,j=x,y,z$ denote the components along three orthogonal coordinate axes, $n(r)$ is a local director, and $S(r)$ is the scalar orientational order parameter referred to previously. The dynamics of the mixture is described by the coupled time-dependent Ginzburg-Landau equations [23–28] for the two order parameters. In the inhomogeneous system under nonequilibrium conditions, spatial variations occur in the two order parameters. The total free energy (F) can be expressed in terms of a local bulk free energy density $f(\phi,S_{ij})$ and the gradients of the two order parameters [26,28,33]:

$$F[\phi,S_{ij}]=\int dr\left[f(\phi,S_{ij})+\frac{K_0}{2}(\nabla\phi)^2+L_0(\partial_i\phi)(\partial_jS_{ij})+\frac{L_1}{2}(\partial_kS_{ij})^2+\frac{L_2}{2}(\partial_iS_{ik})(\partial_jS_{jk})\right], \quad (3.2)$$

where the free energy F and f are dimensionless quantities (divided by k_BT), T is the absolute temperature, k_B is the Boltzmann constant, and K_0, L_0, L_1, L_2 are phenomenological coefficients derived from a mean field theory [26,27].

In this paper we take these coefficients as constant. Equation (2.1) is recovered from the following expression for the bulk free energy density:

$$f(\phi,S_{ij})=\frac{1-\phi}{n_p}\ln(1-\phi)+\frac{\phi}{n_l}\ln\phi+\chi\phi(1-\phi)+\frac{1}{2}A(\phi)S_{ij}S_{ji}-\frac{1}{3}B(\phi)S_{ij}S_{jk}S_{ki}+\frac{1}{4}C(\phi)S_{ij}S_{jk}S_{kl}S_{li}, \tag{3.3}$$

where

$$A(\phi)=\frac{2}{3}\left(1-\frac{\eta}{3}\right)\nu\phi^2, \tag{3.4}$$

$$B(\phi)=\frac{4}{15}\eta\nu\phi^2, \tag{3.5}$$

$$C(\phi)=\frac{1}{27}\eta\nu\phi^2. \tag{3.6}$$

In considering the nonequilibrium equations of motion for our system, we adopt a thermodynamic point of view. The phenomenological equation of motion for the concentration ϕ, which ensures local conservation of material, is given by [3,4]

$$\frac{\partial\phi(r,t)}{\partial t}=\Gamma_\phi\nabla^2\left(\frac{\delta F}{\delta\phi}\right)=\Gamma_\phi\nabla^2\left[\frac{\partial f}{\partial\phi}-K_0\nabla^2\phi-L_0\partial_i\partial_j S_{ij}\right], \tag{3.7}$$

where the thermodynamic force which drives the flux is given by the gradient of the chemical potential $\mu=\delta F/\delta\phi$ and Γ_ϕ is the mobility, assumed constant. On the other hand, for the nonconserved order parameter S_{ij}, we take the local rate of change to be linearly proportional to the local thermodynamic force $\partial F/\partial S_{ij}$ [3,4]. The equation of motion for S_{ij} is then given by

$$\frac{\partial S_{ij}(r,t)}{\partial t}=-\Gamma_S\left(\frac{\delta F}{\delta S_{ij}}+\Lambda(r,t)\delta_{ij}\right)=-\Gamma_S\left[\frac{\partial f}{\partial S_{ij}}-L_0\partial_i\partial_j\phi-L_1\nabla^2 S_{ij}-\frac{L_2}{2}(\partial_i\partial_k S_{kj}+\partial_j\partial_k S_{ki})+\Lambda(r,t)\delta_{ij}\right], \tag{3.8}$$

where the transport coefficients Γ_ϕ and Γ_S are taken as constant. The kinetic equations could in principle be made more general, by writing the Onsager coefficient Γ as a matrix. This would allow one order parameter to be driven by gradients in the chemical potential of the other [26]. However, as this is not the phenomenon under investigation, we set the off-diagonal matrix elements to zero for simplicity. The orientational order parameter evolves in such a way as to lower the free energy, but it must do so subject to the constraint that it remains traceless. The Lagrange multiplier Λ in Eq. (3.8) will be chosen to ensure conservation of the trace of S_{ij} [35].

We study here a linearized analysis of the phase separation kinetics and define variables $\delta\phi(r,t)=\phi(r,t)-\phi_0$ and $\delta S_{ij}(r,t)=S_{ij}(r,t)-S_{ij,0}$, where ϕ_0 and $S_{ij,0}$ are the values of concentration and orientation in the initial homogeneous system, respectively. The equilibrium free energy can be expanded about the initial homogeneous state of the uniform concentration (ϕ_0) and orientational order ($S_{ij,0}$) in the early stage:

$$f(\phi,S_{ij})=f(\phi_0,S_{ij,0})+\left(\frac{\partial f}{\partial\phi}\right)\delta\phi+\left(\frac{\partial f}{\partial S_{ij}}\right)\delta S_{ij}. \tag{3.9}$$

When this expansion is substituted into Eqs. (3.7) and (3.8), linear equations of motion are obtained for $\delta\phi$ and δS_{ij}, with coefficients that depend on first and second derivatives of the bulk free energy density $f(\phi,S_{ij})_0$, which we shall now evaluate.

In this paper we consider thermal quenches from the stable isotropic phase into the nematic unstable region (Nu) and the isotropic unstable region (Iu) in Fig. 1. When the initial homogeneous state is isotropic, we can set $S_{ij,0}=0$. From Eq. (3.3), the required derivatives of f are then given by $(\partial f/\partial S_{ij})_0=0$, and by

$$f_{\phi\phi}\equiv(\partial^2 f/\partial\phi^2)_0=\frac{1}{n_p(1-\phi_0)}+\frac{1}{n_l\phi_0}-2\chi, \tag{3.10}$$

$$f_{\phi S}\equiv(\partial^2 f/\partial\phi\partial S_{ij})_0=0, \tag{3.11}$$

and the matrix of second derivatives with respect to S_{ij} becomes diagonal, with components

$$f_{SS}\delta_{ij}\equiv(\partial^2 f/\partial S_{ij}^2)_0=\frac{2}{3}\nu\phi_0^2(1-n_l\nu\phi_0/3)\delta_{ij}. \tag{3.12}$$

The first derivative $(\partial f/\partial\phi)_0$ is nonzero but, being constant, it is removed by the ∇^2 operator in Eq. (3.7). Thus, substituting Eq. (3.9) into the kinetic equations (3.7) and (3.8) yields the coupled partial differential equations

$$\frac{\partial}{\partial t}\delta\phi(r,t)=\Gamma_\phi[f_{\phi\phi}\nabla^2\delta\phi-K_0\nabla^4\delta\phi-L_0\nabla^2\partial_i\partial_j\delta S_{ij}], \tag{3.13}$$

$$\frac{\partial}{\partial t}\delta S_{ij}(r,t)=-\Gamma_S\left[f_{SS}\,\delta_{ij}\,\delta S_{ij}-L_0\partial_i\partial_j\delta\phi-L_1\nabla^2\delta S_{ij}-\frac{L_2}{2}(\partial_i\partial_k\delta S_{kj}+\partial_j\partial_k\delta S_{ki})+\Lambda\delta_{ij}\right], \tag{3.14}$$

where the indices ij of the first Kronecker δ are not summed over. Note that, for a quench from the isotropic phase as considered here, the only coupling between ϕ and S_{ij} enters through the cross-gradient coefficient L_0.

In the Fourier representation, the differential equations (3.13) and (3.14) become

$$\frac{\partial}{\partial t}\delta\phi(q,t) = -\Gamma_\phi q^2[(f_{\phi\phi}+K_0q^2)\delta\phi(q,t) + L_0 q_i q_j \delta S_{ij}(q,t)], \tag{3.15}$$

$$\frac{\partial}{\partial t}\delta S_{ij}(q,t) = -\Gamma_S\Big\{(f_{SS}\delta_{ij}+L_1q^2)\delta S_{ij}(q,t) + \frac{L_2}{2}[q_iq_k\delta S_{kj}(q,t)+q_jq_k\delta S_{ki}(q,t)] + L_0q_iq_j\delta\phi(q,t)+\Lambda(q,t)\delta_{ij}\Big\}. \tag{3.16}$$

The above equations are valid at early times, when the linearization about the initial (uniform, unoriented) state is valid. Since the initial state is isotropic, the response must be independent of the direction q and so, following Ref. [26], we can define a z axis to be oriented along q, $q_i = q\delta_{iz}$. At linear order, the concentration only couples to the component S_{zz} of the orientational order parameter S_{ij}. As a result, we find

$$\frac{\partial}{\partial t}\delta\phi(q,t) = -a(q)\,\delta\phi(q,t) - b(q)\delta S_{zz}(q,t), \tag{3.17}$$

$$a(q) \equiv \Gamma_\phi(f_{\phi\phi}+K_0q^2)q^2, \tag{3.18}$$

$$b(q) \equiv \Gamma_\phi L_0 q^4, \tag{3.19}$$

for the concentration and

$$\frac{\partial}{\partial t}\delta S_{zz}(q,t) = -\Gamma_S[f_{SS}+(L_1+L_2)q^2]\delta S_{zz}(q,t) - \Gamma_S L_0 q^2\delta\phi(q,t) - \Gamma_S\Lambda(q,t) \tag{3.20}$$

for δS_{zz}. The other diagonal components of the orientational order parameter obey

$$\frac{\partial}{\partial t}\delta S_{xx}(q,t) = -\Gamma_S(f_{SS}+L_1q^2)\delta S_{xx}(q,t) - \Gamma_s\Lambda(q,t), \tag{3.21}$$

$$\frac{\partial}{\partial t}\delta S_{yy}(q,t) = -\Gamma_S(f_{SS}+L_1q^2)\delta S_{yy}(q,t) - \Gamma_s\Lambda(q,t). \tag{3.22}$$

The solution of Eqs. (3.21) and (3.22) for δS_{xx} and δS_{yy} is

$$\begin{aligned}\delta S_{xx}(q,t) &= \delta S_{yy}(q,t)\\ &= \delta S_{xx}(q,0)\exp[-\epsilon(q)t] + \Gamma_S\int_0^t \Lambda(q,t)\exp[-\epsilon(q)(t-t_1)]dt_1,\end{aligned} \tag{3.23}$$

where

$$\epsilon(q) \equiv \Gamma_S(f_{SS}+L_1q^2). \tag{3.24}$$

Note that off-diagonal components of δS_{ij} are decoupled, and simply decay exponentially, with rate constant $\Gamma_S L_1 q^2$, or $\Gamma_S(L_1+L_2)q^2$ if one coordinate index is z.

Adding Eqs. (3.20), (3.21), and (3.22) and demanding tracelessness ($S_{ii}=0$) yields

$$\Lambda(q,t) = -\frac{L_0}{3}q^2\delta\phi(q,t) - \frac{L_2}{3}q^2\delta S_{zz}(q,t). \tag{3.25}$$

Substituting this expression for the Lagrange multiplier into Eq. (3.20), the equation of motion for the component S_{zz} of the orientational order parameter becomes

$$\frac{\partial}{\partial t}\delta S_{zz}(q,t) = -c(q)\,\delta S_{zz}(q,t) - d(q)\,\delta\phi(q,t), \tag{3.26}$$

where

$$c(q) \equiv \Gamma_S\left[f_{SS}+\left(L_1+\frac{2}{3}L_2\right)q^2\right], \tag{3.27}$$

$$d(q) \equiv \frac{2}{3}\Gamma_S L_0 q^2. \tag{3.28}$$

Finally, the linearized coupled equations for $\delta\phi$ and δS_{zz}, Eqs. (3.17), (3.26), are solved, giving

$$\delta\phi(q,t) = u_1(q)\exp[\omega_1(q)t] + u_2(q)\exp[\omega_2(q)t], \tag{3.29}$$

$$\delta S_{zz}(q,t) = u_3(q)\exp[\omega_1(q)t] + u_4(q)\exp[\omega_2(q)t], \tag{3.30}$$

where the growth rates ω_1 and ω_2 are given by

$$\omega_1(q) = \frac{1}{2}[-a(q)-c(q)+\sqrt{(c(q)-a(q))^2+4b(q)d(q)}], \tag{3.31}$$

$$\omega_2(q) = \frac{1}{2}[-a(q)-c(q)-\sqrt{[c(q)-a(q)]^2+4b(q)d(q)}], \tag{3.32}$$

and the four coefficients in Eqs. (3.29) and (3.30) are given, as a function of wave number q, by

$$u_1(q) = \frac{1}{\omega_1(q)-\omega_2(q)}\{-[\omega_2(q)+a(q)]\delta\phi(q,0) + b(q)\delta S_{zz}(q,0)\}, \tag{3.33}$$

$$u_2(q) = \frac{1}{\omega_1(q)-\omega_2(q)}\{[\omega_1(q)+a(q)]\delta\phi(q,0) - b(q)\delta S_{zz}(q,0)\}, \tag{3.34}$$

$$u_3(q) = \frac{1}{\omega_1(q)-\omega_2(q)}\{-[\omega_2(q)+c(q)]\delta S_{zz}(q,0) + d(q)\delta\phi(q,0)\}, \tag{3.35}$$

$$u_4(q)=\frac{1}{\omega_1(q)-\omega_2(q)}\{[\omega_1(q)+c(q)]\delta S_{zz}(q,0) - d(q)\delta\phi(q,0)\}. \quad (3.36)$$

These results can be used to study the time evolution of various structure factors. The structure factor for concentration is defined by

$$S_\phi(q,t)\equiv\langle|\delta\phi(q,t)|^2\rangle, \quad (3.37)$$

and that for the component S_{zz} of the orientational order parameter is given by

$$S_S(q,t)\equiv\langle|\delta S_{zz}(q,t)|^2\rangle. \quad (3.38)$$

Before the quench, the structure factors S_ϕ and S_S have the Ornstein-Zernike form:

$$S_\phi(q,0)=[u_1(q)+u_2(q)]^2=\langle|\delta\phi(q,0)|^2\rangle = \frac{1}{f^0_{\phi\phi}+K_0q^2}, \quad (3.39)$$

$$S_S(q,0)=[u_3(q)+u_4(q)]^2=\langle|\delta S_{zz}(q,0)|^2\rangle = \frac{1}{f^0_{SS}+(L_1+2L_2/3)q^2}, \quad (3.40)$$

where $f^0_{\phi\phi}$, f^0_{SS} are the second derivatives of f before the quench, when we are somewhere above the two-phase region in Fig. 1. We shall take the prequench temperature to be $\tau=1$. So Eqs. (3.39) and (3.40) set the initial conditions ($t=0$).

Equations (3.29) and (3.30) allow the calculation of the structure factor for concentration as measured by small angle light scattering or x-ray scattering. Experimentally, for single component nematics, orientational fluctuations dominate the scattering, although this need not be true for the binary mixtures considered here. For simplicity, we consider only the zz orientational structure factor $S_S(q,t)$ [Eq. (3.38)] although in principle, Eq. (3.23) and the remarks following it could be used to find that of other components of S_{ij}.

IV. RESULTS AND DISCUSSION

In this section we plot some results of the structure factor calculations for the concentration and for the orientation S_{zz} in the case of the thermal quench from the stable isotropic phase ($\tau=1$) into the nematic unstable (Nu) and isotropic unstable regions (Iu) in Fig. 1. We here set $\Gamma_\phi=1$, $\Gamma_S=1$, $K_0=0.4$, $L_0=0.2$, and $L_1=L_2=0.1$ for a typical example. In using dimensionless units, we are measuring length, time, and energy in the characteristic molecular units of the system.

A. Spinodal decomposition induced by concentration fluctuations

It is informative first to consider the behavior of the SD with $L_0=0$. When $L_0=0$, we obtain $b(q)=d(q)=0$ and then the kinetic equations (3.17) and (3.26) have no cross term between concentration and orientation. The equation (3.17) results in the Cahn theory of SD for isotropic solutions [2]. The structure factor for concentration is given by $\langle|\delta\phi(q,t)|^2\rangle=\langle|\delta\phi(q,0)|^2\rangle\exp[-2a(q)t]$. When $f_{\phi\phi}>0$, the amplitude of any concentration fluctuation decreases with time because $a(q)>0$ and so the system is stable. If $f_{\phi\phi}<0$, concentration fluctuations are unstable for the wave vector in the range $0<q<q_0=(-f_{\phi\phi}/K_0)^{1/2}$ and the amplitude of the corresponding modes grows exponentially with time. The structure factor for concentration has a maximum at $q=q_m(=q_0/\sqrt{2})$ and vanishes at all times for $q=0$ because the concentration is conserved [$\int\delta\phi(r)dr=0$]. On the other hand, the structure factor for S_{zz} is given by $\langle|\delta S_{zz}(q,t)|^2\rangle=\langle|\delta S_{zz}(q,0)|^2\rangle\exp[-2c(q)t]$. The eigenvalue $c(q)$ is nonzero at $q=0$ because the orientational order parameter S is not conserved. When $f_{SS}>0$, the amplitude of any orientation fluctuation decreases with time because $c(q)>0$ and the system is stable. If $f_{SS}<0$, orientation fluctuations are unstable for the wave number in the range $0<q<q_1=\{-f_{SS}/[L_1+(2/3)L_2]\}^{1/2}$ and the amplitudes of the corresponding modes grow exponentially with time. The structure factor for orientation decreases with increasing wave number q [23] because the amplitude $c(q)$ monotonically increases with increasing q. The orientation fluctuation with $q=0$ corresponds to a macroscopic fluctuation of a orientational order parameter throughout the system.

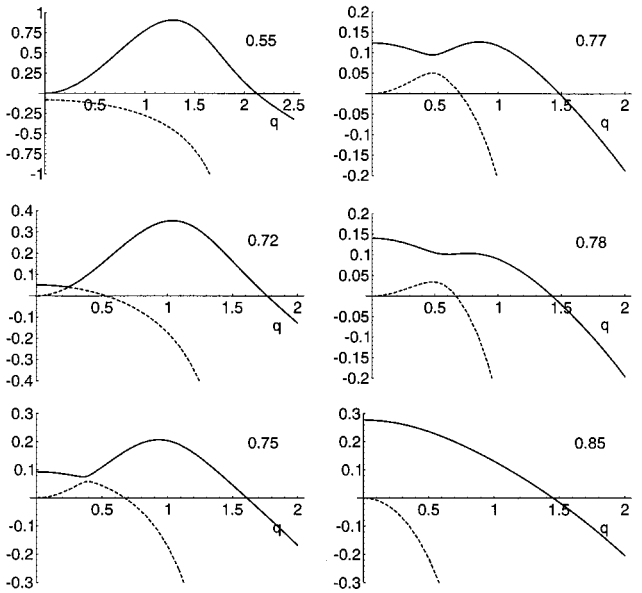

FIG. 2. Two growth rate $\omega_1(q)$ (solid line) and $\omega_2(q)$ (dotted line) are shown against the wave number q. Concentration ϕ_0 of the liquid crystal is varied with fixed temperature $\tau=0.6$.

When L_0 has nonzero values (>0), we have a coupling between fluctuations of concentration and orientation. The structure factors will be affected by this cross term even in the linear regime of the SD studied here. Figure 2 shows the two growth rates $\omega_1(q)$ (solid line) and $\omega_2(q)$ (dotted line) of Eqs. (3.31) and (3.32). The initial concentration ϕ_0 of the liquid crystal is varied, with $\tau=0.6$ after the quench. When $\phi_0=0.55$ in the Iu region, the growth rate $\omega_1(q)$ has positive values in the range $0<q<q_0(=2.21)$ and has a maximum at $q_m=1.3$. This maximum is driven by the instability of the concentration fluctuation, $f_{\phi\phi}<0$. The other eigenvalue

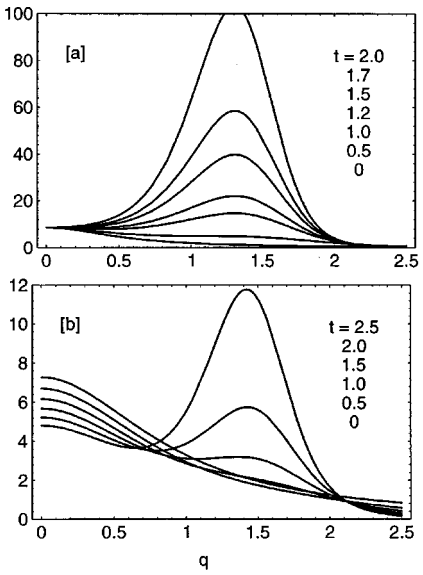

FIG. 3. Temporal evolution of the compositional structure factor (a) S_ϕ and of the orientational structure factor (b) S_S, for the temperature quench into the Iu region (A) ($\tau=0.6,\phi=0.55$) in Fig. 1.

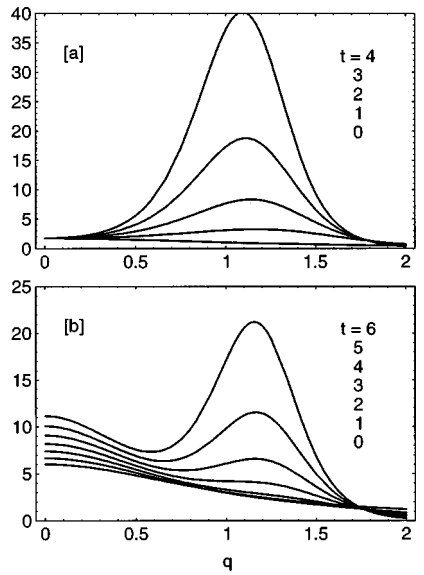

FIG. 4. Temporal evolution of the compositional structure factor (a) S_ϕ and of the orientational structure factor (b) S_S, for the temperature quench into the Nu region (B) ($\tau=0.6,\phi=0.72$) in Fig. 1.

$\omega_2(q)$ has negative values for all q because $f_{SS}>0$. On increasing the concentration, the growth rate $\omega_1(q)$ has two peaks. One is the peak at $q=0$, which is induced by the instability of the orientation fluctuation $f_{SS}<0$ and the other is the peak at q_m, which is driven by the instability of the concentration fluctuation $f_{\phi\phi}<0$. The hybridization of eigenvalues appears at around $\phi_0=0.72$. At $\phi=0.77$, the amplitude of these two peaks becomes equal. Further increasing the concentration of the mesogen, the value of the peak at $q=0$ becomes larger than that at q_m. In the Nu region (C)($\phi_0=0.85$), in which the system is outside the isotropic spinodal curve ($f_{SS}<0$, $f_{\phi\phi}>0$), the growth rate $\omega_1(q)$ decreases with increasing q.

Figures 3(a) and 3(b) show the temporal evolution of the compositional structure factor S_ϕ and of the orientational structure factor S_S, respectively, for the temperature quench into the Iu region ($\tau=0.6,\phi=0.55$) in Fig. 1. The structure factor for concentration has a maximum at q_m which corresponds to the peak wave number of $\omega_1(q)$. With time the corresponding mode grows exponentially and the peak position q_m is invariant. The time evolution of the structure factor S_ϕ is the same as that of the Cahn theory for isotropic SD [2,3]. The structure factor S_S decreases with increasing q at very early times. The amplitude of the peak at $q=0$ decreases with time because $f_{SS}>0$. With time another peak appears in the S_S curve, corresponding to the peak at q_m in $\omega_1(q)$, and the orientation fluctuation grows exponentially. In this quench, the concentration fluctuation initially induces the SD and the orientational ordering within the domains subsequently takes place due to the coupling between the two order parameters as time progresses.

Figure 4 shows the structure factors for the temperature quench into the Nu region (B)($\tau=0.6,\phi=0.72$) in Fig. 1. In the Nu region (B), the system is unstable with respect to both orientational order ($f_{SS}<0$) and concentration ($f_{\phi\phi}<0$). The structure factor S_ϕ, Fig. 4(a), has a maximum at the wave number q_m at which $\omega_1(q)$ has a peak. The corresponding mode grows exponentially with time. As shown in Fig. 4(b), the structure factor S_S decreases with increasing q at very early stages. The amplitude of the peak at $q=0$ in S_S increases with time because $f_{SS}<0$. As time increases, another peak appears in the S_S curve at q_m, which corresponds to the maximum of $\omega_1(q)$. The orientation fluctuations are induced by the concentration fluctuations. The corresponding mode grows exponentially with time, so at later times the fastest growing mode (at q_m) is dominant.

Figure 5 shows the structure factors for the temperature quench with $\tau=0.6$, $\phi=0.78$, which is also in the Nu region (B) of Fig. 1. The structure factor S_ϕ [Fig. 5(a)] has a maximum and the corresponding mode grows exponentially. However, the peak position q_m slightly shifts to lower values of q with time (see Fig. 8). The structure factor S_S [Fig. 5(b)]

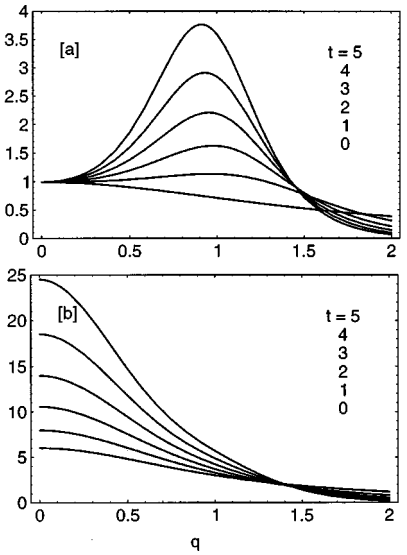

FIG. 5. Temporal evolution of the compositional structure factor (a) S_ϕ and of the orientational structure factor (b) S_S, for the temperature quench into the Nu region (B) ($\tau=0.6,\phi=0.78$) in Fig. 1.

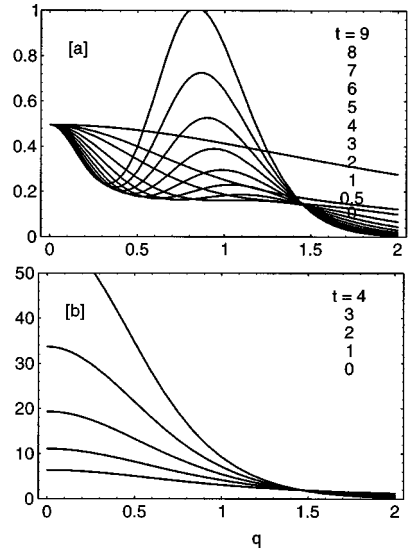

FIG. 6. Temporal evolution of the compositional structure factor (a) S_ϕ and of the orientational structure factor (b) S_S, for the temperature quench into the Nu region (C) ($\tau=0.6$, $\phi=0.85$) in Fig. 1.

decreases with increasing q because the amplitude of the growth rate $\omega_1(q)$ at $q=0$ is larger than that at q_m as shown in Fig. 2.

B. Spinodal decomposition induced by orientation fluctuations

Further increasing the initial concentration of mesogen, the orientational fluctuation becomes dominant. Figure 6 shows the temporal evolutions of the structure factors for a temperature quench into the Nu region (C) ($\tau=0.6,\phi=0.85$), where the system is initially unstable with respect to orientational order parameter ($f_{SS}<0$) and metastable with respect to concentration ($f_{\phi\phi}>0$). In the very early stages, the concentration fluctuation becomes weak with time because $f_{\phi\phi}>0$. However, the orientational fluctuations grow exponentially with time because $f_{SS}<0$. Further increasing time, a peak in S_ϕ appears and shifts to lower values of the wave number. There is no longer any time stage in which the peak position in S_ϕ is invariant, which was predicted by Cahn's linearized theory for isotropic SD in the early stages [2,3]. The instability of the orientational ordering initially induces the SD and the concentration fluctuation is induced by the coupling between the two order parameters. The change of the peak wave number in S_ϕ can be understood by

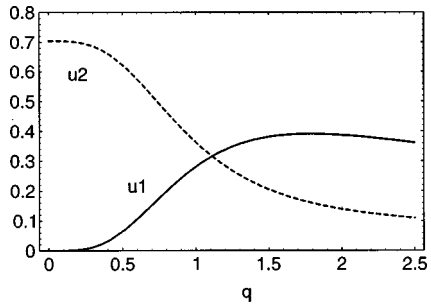

FIG. 7. The coefficients $u_1(q)$ and $u_2(q)$ in the structure factor S_ϕ plotted as a function of the wave number q for the quench ($\tau=0.6,\phi=0.85$).

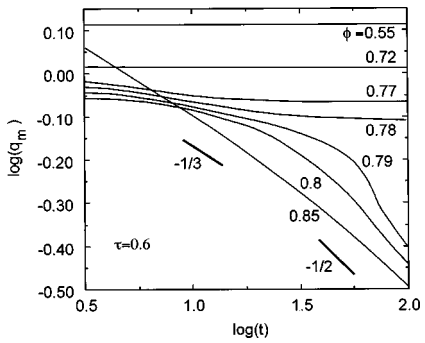

FIG. 8. Temporal evolutions of the scattering wave number q_m at which the compositional structure factor has a maximum. The initial concentration is varied at fixed τ.

examining the two coefficients $u_1(q)$ and $u_2(q)$ as shown in Fig. 7. With time, the term $u_2(q)\exp[\omega_2(q)t]$ in Eq. (3.29) tends towards zero because $\omega_2(q)$ is everywhere negative as shown in Fig. 2. However, the product of $u_1(q)$ and an exponential containing $\omega_1(q)t$ has a peak because the value of $u_1(q)$ increases from zero (see Fig. 7), while $\omega_1(q)$ decreases from a positive value with increasing q. As time increases, the factor $\exp[\omega_1(q)t]$ becomes large, but $u_1(0)=0$, and so the peak in the S_ϕ shifts to the lower values of the wave number q.

When the orientation fluctuation is dominant, $f_{SS}\ll f_{\phi\phi}$, we have $\omega_1(q)\gg\omega_2(q)$ and $-c(q)\gg -a(q)$ as shown in Fig. 2. Then we can neglect the $\omega_2(q)$ and $a(q)$ terms in Eqs. (3.29) and (3.31). The structure factor S_ϕ can be approximated by

$$S_\phi(q,t)\approx u_1^2(q)\exp[2\omega_1(q)t], \tag{4.1}$$

where

$$\omega_1(q)\approx\frac{1}{2}\left[-\Gamma_S\left[f_{SS}+\left(L_1+\frac{2}{3}L_2\right)q^2\right]+\sqrt{\Gamma_S^2\left[f_{SS}+\left(L_1+\frac{2}{3}L_2\right)q^2\right]^2+\frac{8}{3}\Gamma_S\Gamma_\phi L_0^2 q^6}\right], \tag{4.2}$$

$$u_1^2(q)\approx\left[\frac{b(q)}{\omega_1(q)}\right]^2 S_S(q,0). \tag{4.3}$$

The peak wave number q_m is given by $(\partial S_\phi/\partial q)_{q_m}=0$:

$$t=-\frac{1}{u_1(q_m)}\left(\frac{\partial u_1(q)}{\partial q}\right)_{q_m}\Bigg/\left(\frac{\partial\omega_1(q)}{\partial q}\right)_{q_m}. \tag{4.4}$$

Substituting Eqs. (4.2) and (4.3) into (4.4), we obtain

$$t\approx\frac{1}{\omega_1(q_m)}. \tag{4.5}$$

At large q, the growth rate $\omega_1(q)$ is governed, in our minimal model, by the $L_0^2q^6$ term in the square root of Eq. (4.2) and so we obtain the growth law

$$q_m\sim t^{-1/3}. \tag{4.6}$$

This describes a regime where the growth of droplets is driven by the cross term L_0 between the local gradients of the two order parameters. At intermediate q, the $\Gamma_S[L_1+(2/3)L_2]q^2$ term in Eq. (4.2) becomes dominant and so the growth law is given by

$$q_m \sim t^{-1/2}. \tag{4.7}$$

At small q, we find

$$q_m \sim t^{-1}, \tag{4.8}$$

because the $\Gamma_S f_{SS}[L_1+(2/3)L_2]q^2$ term in the square root of Eq. (4.2) becomes dominant. When the peak wave number q_m is shifted to smaller values with time, the time dependence of the average domain size R and of the wave number q_m is given by

$$R = 2\pi/q_m \sim t^{\alpha}, \tag{4.9}$$

where, in our model, the dynamical exponent α changes, with increasing time, from 1/3 through 1/2 to 1. If a more elaborate model were used, incorporating terms of higher order in q or perhaps off-diagonal components of the Onsager mobility matrix, then the values of the exponent α might be modified. Nevertheless, we have demonstrated what we expect to be generic qualitative behavior: that the scattering peak of the orientation-induced SD evolves continuously to lower wave numbers. Hence the average domain size is time dependent in the Nu region (C), in spite of the linearized analysis of the TDLG.

This means that the SD is advanced by the instability of the orientational ordering and no longer follows Cahn's theory which predicts no shift in the peak of S_ϕ in the early stages. Recent simulations indeed suggest that the coupling of phase separation and ordering leads to a faster onset of phase separation [28]. Nakai *et al.* have experimentally observed the phase separations of poly (ethylene terephthalate)–liquid-crystal mixtures and reported the characteristic length initially follows the power law 1/3, then crosses over to the 1 regime [20]. If we thermally quench into the Nu region (C), the growth of domains takes place sooner than in the usual SD of the isotropic phase separations.

To summarize these results of our linearized analysis, we show in Fig. 8 the values of q_m for the density structure factor S_ϕ for various initial concentrations ϕ_0. In the Iu region (A), the peak wave number q_m is invariant during the early stages of the SD. On increasing the initial concentration, we find that the scattering peak shifts to the lower values with time. When $\phi_0 = 0.85$ (region C), the scattering peak for S_ϕ changes as $t^{-1/3}$ (the average domain size increases as $t^{1/3}$ even in the early stages). The instability of the orientational ordering induces the concentration fluctuation through the coupling between two order parameters.

C. Simulations in one dimension

To further understand our analytical results, nonlinear coupled differential equations were simulated in one spatial dimension with periodic boundary conditions. A traceless tensor order parameter cannot be defined in one dimension, but a reasonable extension of the model to 1D is to use the bulk free energy density of Eq. (2.1) with square gradient terms for the concentration ϕ and the *scalar* order parameter S. We then evolve the order parameters according to the nonlinear equations of motion

$$\dot{\phi} = \Gamma_\phi \nabla^2 \frac{\delta F}{\delta \phi}$$

$$\dot{S} = -\Gamma_S \frac{\delta F}{\delta S},$$

which have *the same linear regime* [Eqs. (3.17, 3.26)] as the three-dimensional, tensorial equations of motion (3.7), (3.8). The time step and grid spacing are $\Delta t = 0.001$ and $\Delta z = 0.5$, respectively, and 100 grid points were used. The initial conditions for the concentration $\phi(z)$ and the scalar orientational order parameter $S(z)$ at each lattice point are given by random numbers distributed uniformly in $\phi(z) = \phi_0 \pm 0.02$ and $S(z) = \pm 0.02$, respectively. [This choice is computationally expedient, and leads to a white-noise power spectrum, somewhat different from the Ornstein-Zernike form of Eqs. (3.39) and (3.40).] Initially, the system is in an isotropic phase. Figures 9, 10, and 11 show the results of simulations for temperature quenches from the isotropic state to $\tau = 0.6$ with $\phi_0 = 0.55$, $\phi_0 = 0.77$, and $\phi_0 = 0.85$, respectively. The solid (dotted) line shows the concentration (scalar orientation order parameter) profile. In the case of region (A), with $\phi_0 = 0.55$ [Fig. 9], we first observe the concentration fluctuation

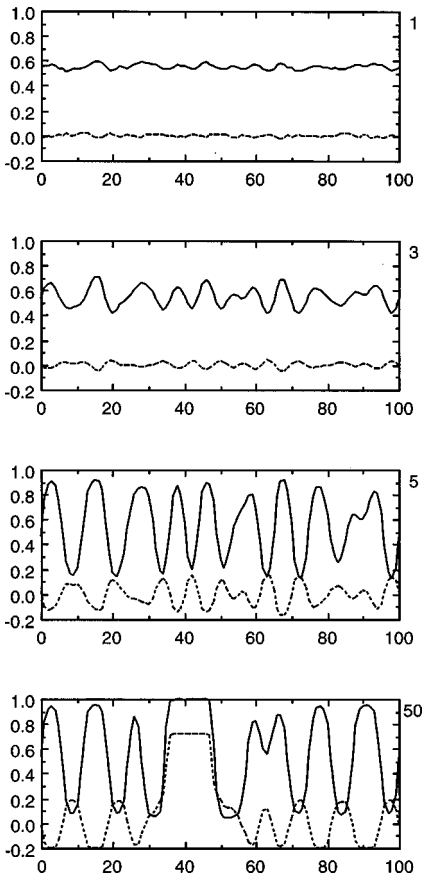

FIG. 9. Time evolution of the compositional (solid line) and orientational (dotted line) order parameters for the temperature quench ($\tau = 0.6, \phi = 0.55$) in Fig. 1.

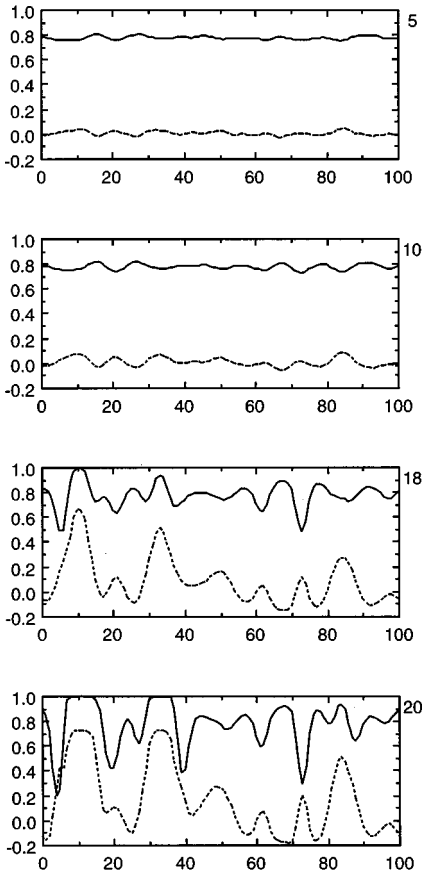

FIG. 10. Time evolution of the compositional (solid line) and scalar orientational (dotted line) order parameters for the temperature quench ($\tau=0.6,\phi=0.77$) in Fig. 1.

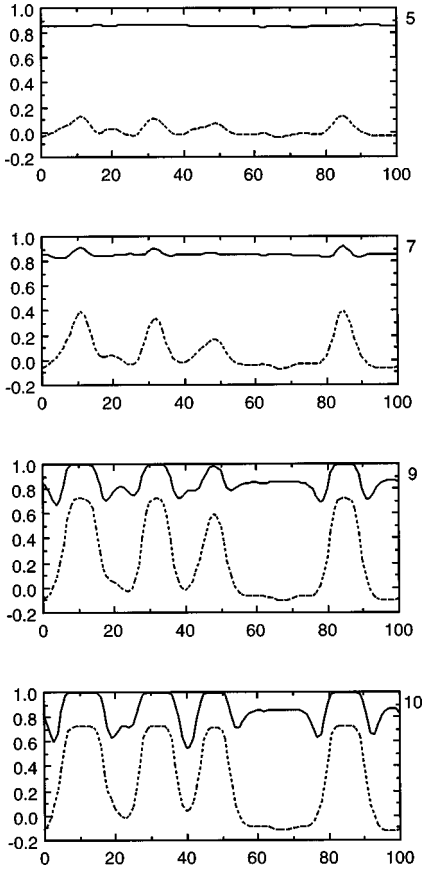

FIG. 11. Time evolution of the compositional (solid line) and orientational (dotted line) order parameters for the temperature quench ($\tau=0.6,\phi=0.85$) in Fig. 1.

in the early stage ($t=1$) and the isotropic domains appear. With time the concentration fluctuation and the orientational fluctuation within the domains grow ($t=3$). At the late stage ($t=50$), we observe the coarsening process. In region (B), at $\phi_0=0.77$ [Fig. 10], fluctuations in both order parameters begin to grow from about the same time ($t=5$). The size of the domains becomes large earlier than in region (A). In the case of $\phi_0=0.85$ [region (C), Fig. 11], we first observe the orientation fluctuations in the early stage ($t=5$), but the system is still isotropic. As time increases, the orientation fluctuations become large and induce concentration fluctuations. The size of the domains grows with time. At $t=7$, the interior of some domains is in a nematic phase. On increasing the concentration of liquid crystal, the growth of droplets takes place in the earlier stages of the SD.

These simulations are consistent with the analytical results. They show how the phase separation dynamics in polymer–liquid-crystal mixtures is driven by the competition between phase separation and nematic ordering. On increasing the concentration of liquid crystal, the instability of the orientational ordering becomes dominant and the mechanism of the SD is changed from concentration fluctuation-induced SD to orientation fluctuation-induced SD. The cross term between gradients plays a significant role in the early stage SD.

V. CONCLUSION

We have studied the early stages of spinodal decomposition (SD) in polymer–liquid-crystal mixtures by solving linearized time-dependent Landau-Ginzburg equations for concentration (conserved order parameter) and orientation (nonconserved order parameter). The theory takes into account a cross term between concentration and orientation gradients. This term plays a significant role in the early stages of the SD. We calculated the structure factor for concentration and for orientation in the thermal quenches from the stable isotropic phase into the Iu or Nu region. We find two distinct growth mechanism in the SD. One is the concentration fluctuation-induced SD in the Iu region. In this case the behavior of the SD follows Cahn's linearized theory which means no shift in the peak of the compositional structure factor is observed in the early stage. The other growth mechanism is a SD driven by the instability with respect to orientational order in the Nu region (C). In this case, the peak position q_m in the compositional structure factor shifts to lower values of the wave number with time. Our reasonable minimal model predicts that the mean radius of domains initially grows as $t^{1/3}$, though this power may be nonuniversal. There is no longer the time stage predicted by the Cahn linearized theory. On increasing the concentration of the mesogens, the behavior of the SD is changed from the concentration fluctuation- to orientation fluctuation-induced SD. Though we have performed a linear analysis of the phase

separation in polymer–liquid-crystal mixtures, these results will also be useful to understand other nematic systems including semiflexible polymers, liquid-crystalline polymers, and rodlike colloids. The main conclusions were confirmed by a numerical solution of appropriate nonlinear equations of motion in one dimension.

ACKNOWLEDGMENTS

We are grateful to Professor Alan Bray for helpful discussions. R.M.L.E. acknowledges The Royal Society of Edinburgh for financial support.

[1] J. D. Gunton, M. S. Miguel, and P. S. Sahni, in *Phase Transitions and Critical Phenomena*, edited by C. Domb and J. L. Lebowitz (Academic, London, 1983).
[2] J.W. Cahn, Trans. Metall. Soc. AIME **242**, 166 (1968).
[3] *Solids Far from Equilibrium*, edited by J. S. Langer (Cambridge University Press, New York, 1992), Chap. 13.
[4] P. M. Chaikin and T. C. Lubensky *Principles of Condensed Matter Physics* (Cambridge University Press, New York, 1995).
[5] I.M. Lifshitz and V.V. Slyozov, J. Phys. Chem. Solids **19**, 35 (1961).
[6] A.N. Kolmogorov, Bull. Acad. Sci. USSR, Phys. Ser. **3**, 355 (1937).
[7] *Liquid Crystalline and Mesomorphic Polymers*, edited by V. P. Shibaev and L. Lam (Springer-Verlag, New York, 1993).
[8] *Liquid Crystals in Complex Geometries*, edited by G. P. Crawford and S. Zumer (Taylor & Francis, London, 1996).
[9] B. Kronberg, I. Bassignana, and D. Patterson, J. Phys. Chem. **82**, 1714 (1978).
[10] A. Dubaut, C. Casagrande, M. Veyssie, and B. Deloche, Phys. Rev. Lett. **45**, 1645 (1980).
[11] H. Orendi and M. Ballauff, Liq. Cryst. **6**, 497 (1989).
[12] W. Ahn, C.Y. Kim, H. Kim, and S.C. Kim, Macromolecules **25**, 5002 (1992).
[13] F. Brochard, J. Jouffroy, and P. Levinson, J. Phys. France **45**, 1125 (1984).
[14] M. Ballauff, Mol. Cryst. Liq. Cryst. **136**, 175 (1986).
[15] R. Holyst and M. Schick, J. Chem. Phys. **96**, 721 (1992).
[16] C. Shen and T. Kyu, J. Chem. Phys. **102**, 556 (1995).
[17] T. Kyu and H.W. Chiu, Phys. Rev. E **53**, 3618 (1996).
[18] A. Matsuyama and T. Kato, J. Chem. Phys. **105**, 1654 (1996); **108**, 2067 (1998); Phys. Rev. E **59**, 763 (1999).
[19] C. Casagrande, M. Veyssie, and C.M. Knobler, Phys. Rev. Lett. **58**, 2079 (1987).
[20] A. Nakai, T. Shiwaku, W. Wang, H. Hasegawa, and T. Hashimoto, Macromolecules **29**, 5990 (1996); Polymer **37**, 2259 (1996).
[21] T. Shimada, M. Doi, and K. Okano, J. Chem. Phys. **88**, 7181 (1988).
[22] A. Ten Bosch, J. Phys. II **1**, 949 (1991).
[23] K.R. Elder, F. Drolet, J.M. Kosterlitz, and M. Grant, Phys. Rev. Lett. **72**, 677 (1994).
[24] J.R. Dorgan, J. Chem. Phys. **98**, 9094 (1993).
[25] H.W. Chiu and T. Kyu, J. Chem. Phys. **110**, 5998 (1999).
[26] A.J. Liu and G.H. Fredrickson, Macromolecules **29**, 8000 (1996); **26**, 2817 (1993).
[27] J. Fukuda, Phys. Rev. E **58**, R6939 (1998); **59**, 3275 (1999).
[28] A.M. Lapena, S.C. Glotzer, A.S. Langer, and A.J. Liu, Phys. Rev. E **60**, R29 (1999).
[29] M. Doi and S. F. Edwards, *Theory of Polymer Dynamics* (Academic, New York, 1986).
[30] P. J. Flory, *Principles of Polymer Chemistry* (Cornell University, Ithaca, 1953).
[31] W. Maier and A. Saupe, Z. Naturforsch. A **14a**, 882 (1959).
[32] P. G. de Gennes and J. Prost, *The Physics of Liquid Crystals*, 2nd ed. (Oxford Science, London, 1993).
[33] P. Sheng and E. B. Priestley, in *Introduction to Liquid Crystals*, edited by E. B. Priestley, P. J. Wojtowicz, and O. Sheng (Plenum Press, New York, 1979), Chap. 10.
[34] Y. Lansac, F. Fried, and P. Maissa, Phys. Rev. E **52**, 6227 (1995).
[35] In Ref. [26], tracelessness was achieved by explicitly removing the associated degree of freedom from the equations of motion, rather than by the Lagrange multiplier method, which we find more convenient.